J. Condensed Matter Nucl. Sci. 3 (2010) 41–49

Research Article

Secondary Neutron Yield in the Presence of Energetic Alpha Particles in PdD

Peter L. Hagelstein *

Research Laboratory of Electronics, Massachusetts Institute of Technology, Cambridge, MA 02139, USA

Abstract

It has been proposed that energy can be released in the Fleischmann–Pons experiment as energetic alpha particles in aneutronic fusion reactions. In this scenario, the energetic alpha particles could be "hidden" since they have a relatively short range in PdD. We evaluate the yield of secondary neutrons which result from deuteron–deuteron fusion reactions from energetic deuterons produced in collisions with energetic alpha particles.

Keywords: Secondary neutron yield, Fleischmann–Pons effect, Aneutronic fusion, Correlation of excess power and neutrons

1. Introduction

In some recent meetings in mid-2009 on excess heat in the Fleischmann–Pons experiment, a review of experimental results was presented for scientists outside of the field. In general, the response was one of astonishment, as might have been predicted. When the discussion turned to the question of mechanism, it quickly became clear how some very good physicists from outside the field viewed the theoretical possibilities. The only possibility worthy of consideration according to them were scenarios in which two deuterons somehow managed to come together to form an alpha particle, which carried of a significant fraction of the reaction energy. If the process were assumed to happen sufficiently deep within the cathode, then they would not make it out of the cathode since the mean free path is relatively short. As a result, these energetic alpha particles would be "hidden".

The difficulty with this kind of proposal was recognized previously by Takahashi and coworkers [1], who noted that energetic alpha particles would give rise to secondary radiation such as neutrons and X-rays. As such, it becomes difficult to "hide" a large number of energetic alpha particles.

We are interested in this work in the quantification of this argument. Fast alpha particles can collide with deuterons and produce neutrons through the inelastic ^{4}He(d,np)^{4}He reaction. To be observable, the alpha energy must be above

*E-mail: plh@mit.edu

7 MeV. Much more likely is secondary neutron production which occurs after an energetic alpha particle collides with a deuteron, producing a less energetic deuteron which can then produce a neutron through the ^{2}H(^{2}H,n)^{3}He reaction. In order to understand quantitatively the yield of neutrons due to energetic alpha particles, one first has to understand the yield of energetic deuterons. Then, one needs the neutron yield as a function of energy for energetic deuterons. We describe below computations leading to the determination of the secondary neutron yield for energetic alpha particles through this mechanism.

Accurate values for the stopping power of alpha particles are readily available, and we are able to compute the energy loss over the range numerically. Given results for the incremental alpha particle energy along its trajectory, all that we need is an estimate for the scattering cross section between the alpha particle and a deuteron, from which we can estimate the yield of secondary neutrons from deuteron-deuteron fusion reactions. In a previous manuscript [2] we have computed the yield of energetic deuterons in PdD and in D_2O, which we can use for the computations discussed here.

2. Impact parameter model for scattering

To proceed, we consider the calculation of the secondary neutron production cross section in a classical impact parameter approximation. We assume that an alpha particle is incident on a deuteron with an energy E in the lab frame. The cross section in this model is expressed as

$$\sigma(E) \;=\; \int_0^\infty Y[E_{\rm d}(E,b)]\,2\pi b\;\,{\rm d}b. \tag{1}$$

Here, b is the impact parameter, which can take on all values between 0 and ∞. The contribution to the secondary neutron production cross section is weighted by the secondary neutron yield Y given the scattered deuteron energy $E_{\rm d}$. The scattered deuteron energy is a function of the initial alpha particle energy E and the impact parameter b. If we have a parameterization for the neutron yield Y, then it is possible to estimate this cross section by doing a set of classical path calculations at each alpha particle energy. This is the approach that we have used.

2.1. Potential model

For the classical path calculation, we have used a combination of a screened Coulomb potential and a hard core Woods–Saxon potential

$$V(r) \;=\; \frac{Z_\alpha Z_{\rm d} e^2}{r}{\rm e}^{-r/D_s} - V_0\frac{1}{{\rm e}^{(r-r_0)/a}+1}. \tag{2}$$

We have used one of the Woods–Saxon potentials from Kambara et al. [3], which is defined by

$$V_0 \;=\; 84.5\ {\rm MeV} \;-\; E_{\rm r}, \qquad r_0 \;=\; 1.15\ {\rm fm}, \qquad a_0 \;=\; 0.7\ {\rm fm}, \tag{3}$$

where $E_{\rm r}$ is the relative energy in MeV.

2.2. Screening

From low-energy beam experiments, we know that screening is important for deuteron–deuteron fusion reactions [4]. Consequently, we would also expect that screening should also be important for alpha–deuteron scattering. Unfortunately, we are not aware of any experimental observations that would be helpful in the selection of a screening energy

relevant for alpha–deuteron elastic scattering. There are some beam experiments for reactions with ^{3}He and deuterons [5,6] which show some increase in the screening energy, but these experiments did not make use of metal deuteride targets which show large screening effects in other experiments.

We decided to match the screening length to the deuteron–deuteron case using the screening energy ($U_e = 800$ eV) of Raiola et al. [4] (note that there is some spread in the experimental results for the screening energy for PdD samples [7]). A screening energy U_e of 1600 eV for energetic alpha particles in PdD leads to a screening length for alpha–deuteron collisions that is matched to the deuteron-deuteron experimental results in PdD.

Note also that this relatively large screening energy results for alpha–deuteron collisions results in a reduction in the in the Rutherford scattering cross section, and an increase in the deuteron–deuteron fusion yield. We were not able to find an experimental result on the screening energy for D_2O, so we used 25 eV.

2.3. Classical path calculation

The trajectories are computed in the lab frame according to

$$M_1 \frac{d^2\mathbf{r}_1}{dt^2} = -\nabla_1 V, \tag{4}$$

$$M_2 \frac{d^2\mathbf{r}_2}{dt^2} = -\nabla_2 V. \tag{5}$$

We used a simple second-order discretization (the Störmer–Verlet method [8])

$$M \frac{\mathbf{r}_{j+1} - 2\mathbf{r}_j + \mathbf{r}_{j-1}}{\Delta t^2} = -(\nabla V)_j \tag{6}$$

with a fixed (small) timestep Δt. Below 1 MeV, the computations are "easy" since the scattering is primarily Rutherford scattering with a relatively weak Coulomb potential. Above 1 MeV, the Coulomb barrier can be penetrated in the classical problem, so that the full force of the Woods–Saxon potential is felt. In this region, a shorter timestep needs to be used. Rather than put in the effort to make use of a more sophisticated numerical approach, we just used more timesteps. In all cases, energy conservation could be verified to at least six digits in the numerical solutions.

2.4. Integration over the impact parameter

We used cubic interpolation combined with local Gaussian integration to obtain a reliable numerical integration over the impact parameter. While Rutherford scattering can produce an increase in the deuteron energy at large impact parameter, the associated yield function may not be large. As a result, the contributions from large b are damped exponentially.

3. Parameterization of the yield functions

In order to compute the secondary neutron yield following elastic scattering with an alpha particle, we require a computation of the yield function for the different deuteron energies. We considered this problem previously [2]. It is convenient to fit the resulting neutron yield as a function of deuteron energy, in order to facilitate the calculation of the secondary neutron cross section.

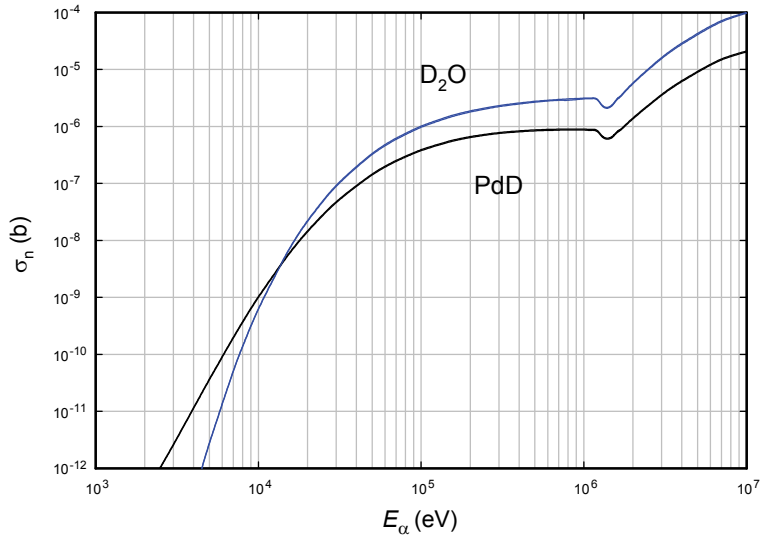

Figure 1. Secondary neutron cross section as a function of alpha particle energy (eV) for alpha particles in PdD and in D_2O.

3.1. Deuteron yield in PdD

In the case of energetic deuterons in PdD, we fit the neutron yield function according to

$$\ln Y = \frac{w}{x^3} + \frac{y}{x^2} + \frac{z}{x} + a + bx + cx^2 + dx^3 \tag{7}$$

with

$$x = \ln\left(\frac{E}{1\text{ eV}}\right) \tag{8}$$

and

$$\begin{aligned} w &= -537226.0, \qquad y = 355399.0, \qquad z = -94344.8, \\ a &= 12753.2, \qquad b = -937.761, \\ c &= 35.5573, \qquad d = -0.546338. \end{aligned} \tag{9}$$

3.2. Deuteron yield in D_2O

In the case of energetic deuterons in D_2O, we fit the neutron yield to the same function using

$$w = -117361.0, \qquad y = 88477.9, \qquad z = -28527.9,$$

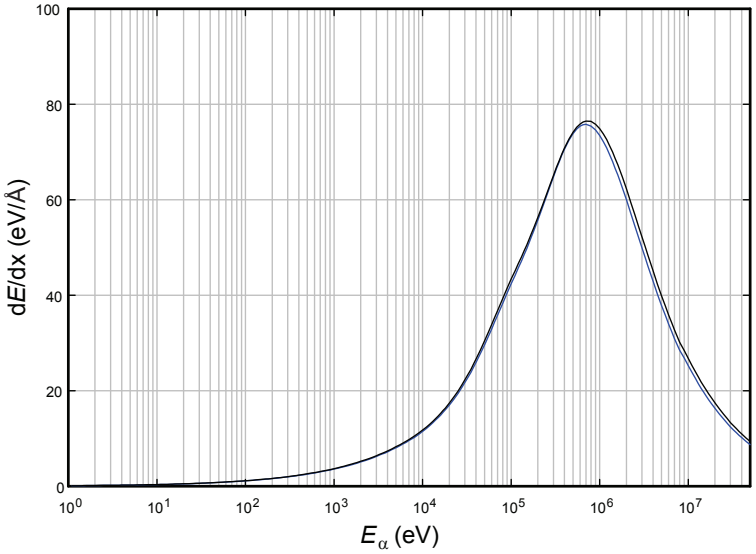

Figure 2. Stopping power for alpha particles in in Pd (black) and in PdD (blue) from SRIM2008.

$$a = 4502.29, \qquad b = -375.23,$$
$$c = 15.7547, \qquad d = -0.262152. \tag{10}$$

These fits were constructed using data between 500 eV and 10 MeV.

4. Cross section for secondary neutron emission

The cross section that results from the impact parameter calculation is shown in Fig. 1 for alpha particles in PdD and in D_2O. Three different regions are apparent in the cross section. Below about 1 MeV, Rutherford scattering is dominant, which when combined with the deuteron-deuteron fusion yield function produces a gently sloping cross section which decreases at lower energy. Above about 1.5 MeV, the alpha–deuteron scattering becomes increasingly dominated by the nuclear interaction potential at small impact parameter, which is favored in the impact parameter integration since hard core scattering produces more energetic deuterons with a higher yield function. Finally, between 1 and 1.5 MeV there is a dip in the cross section. This is a consequence of the presence of trajectories at small impact parameter where the pushing of the Coulomb potential is balanced by the pulling of the nuclear potential, which gives rise to a region where the deuteron energy is too small to cause significant fusion reactions.

The cross section for alpha particles in D_2O is larger at high alpha particle energy because the yield function for secondary neutron production is greater, due to the larger range of deuterons in heavy water as compared to PdD. The cross section for alpha particles in PdD is larger at low energy due to the much stronger screening effects in PdD as compared to D_2O.

5. Stopping power and range of alpha particles in PdD and in D_2O

We have used the SRIM-2008 code of J. F. Ziegler, J. P. Biersack and U. Littmark to compute the stopping power of energetic alpha particles in PdD and in D_2O (see Figs. 2 and 3). The stopping power can be used to compute the alpha

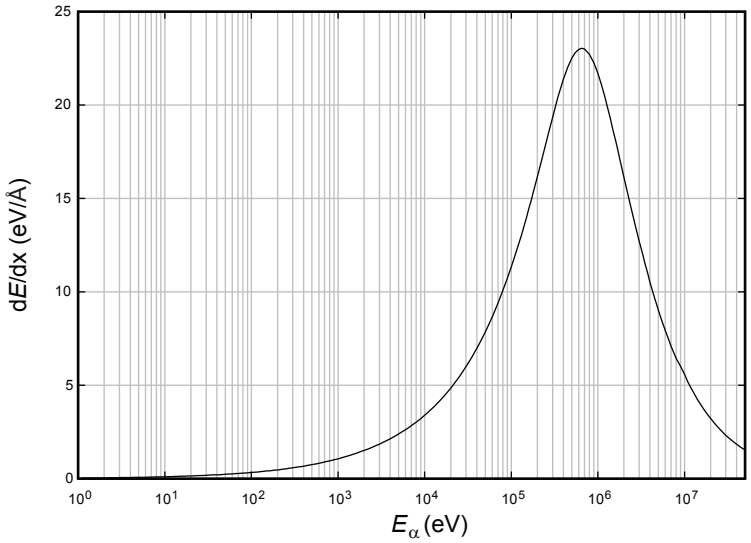

Figure 3. Stopping power for energetic alpha particles in D_2O from SRIM2008.

particle range using

$$R(E) \;=\; \int_0^E \left(\frac{\mathrm{d}E}{\mathrm{d}x}\right)^{-1} \mathrm{d}E. \tag{11}$$

We show the resulting alpha particle range in Fig. 4.

6. Yield of secondary neutrons

We can use the secondary neutron cross section and the stopping power to calculate the yield of secondary neutrons, by integrating the incremental yield over the alpha particle trajectory

$$Y(E) \;=\; \int_0^{R(E)} N_\mathrm{d}\sigma[E(x)]\;\mathrm{d}x. \tag{12}$$

The results for alpha particles in PdD and in D_2O are shown in Fig. 5. We see that the yield is higher in D_2O at high energies, due to the weaker stopping power of D_2O.

In order to compare with experiment, we require the quantity Y/E. This is shown in units of n/J in Fig. 6. At the lower energies one sees that the number of secondary neutrons per unit energy is higher in PdD due to the screening.

7. Sensitivity of yield to screening energies

Of interest in the interpretation of experimental results is the question of the sensitivity of the secondary neutron yield to the model used. In our case, we have two screening parameters with varying degrees of uncertainty. In the case of deuteron-deuteron collisions, measurements of the screening energy has yielded values between about 300 and 800 eV.

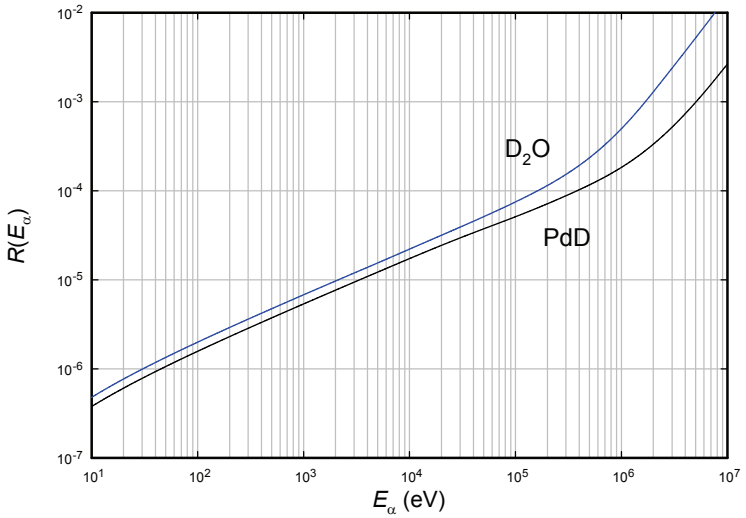

Figure 4. Range of energetic alpha particles in PdD (lower curve) and in D_2O (upper curve).

As mentioned above, we do not have results for the screening energy for alpha–deuteron collisions. As a result, it makes sense to explore the sensitivity of the secondary neutron yield to different assumptions about the two screening energies.

In Fig. 7, we show a close up of results where we have used different values for the two screening energies. In this figure, we see three bands of three curves each. The black, blue, and red curves use deuteron–deuteron screening

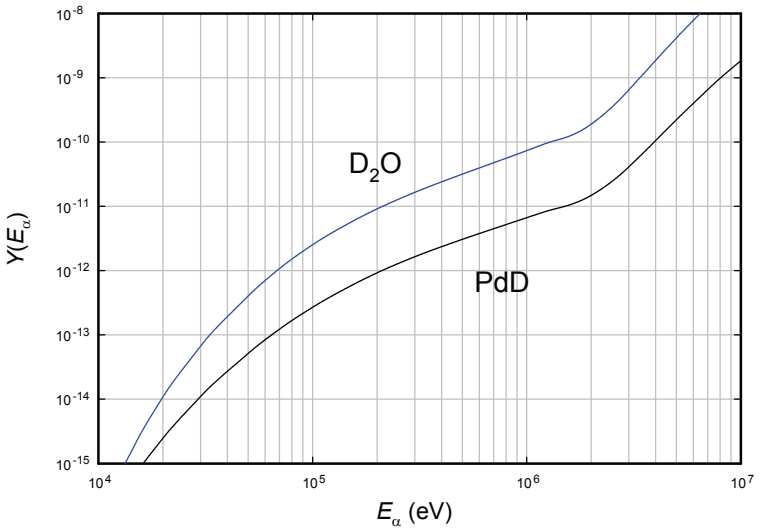

Figure 5. Yield of secondary neutrons in PdD (lower curve) and in D_2O (upper curve).

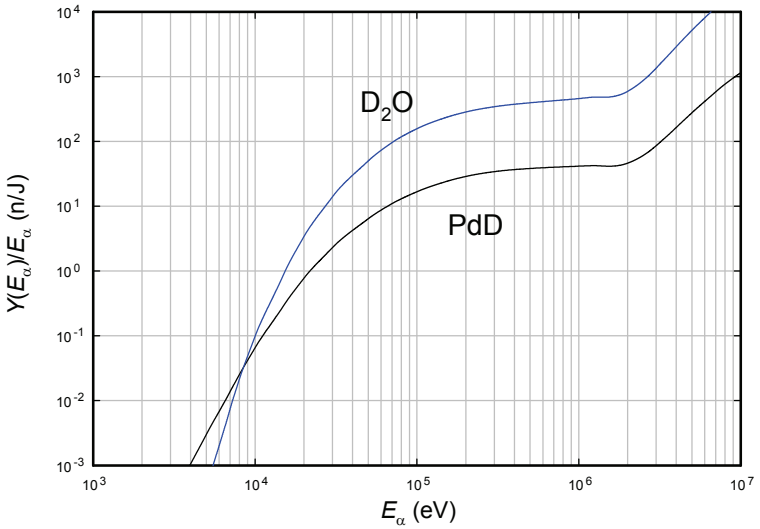

Figure 6. Number of secondary neutrons per joule in PdD (lower curve) and in D_2O (upper curve).

energies $U_e(\mathrm{dd})$ of 0, 400 and 800 eV, respectively. The three different curves within each band have alpha–deuteron screening energies $U_e(\alpha\mathrm{d})$ of 0, 800 and 1600 eV, where increasing screening energy reduces the yield. We see that the yield is most sensitive to the deuteron–deuteron screening energy, and that the spread in the experimental values

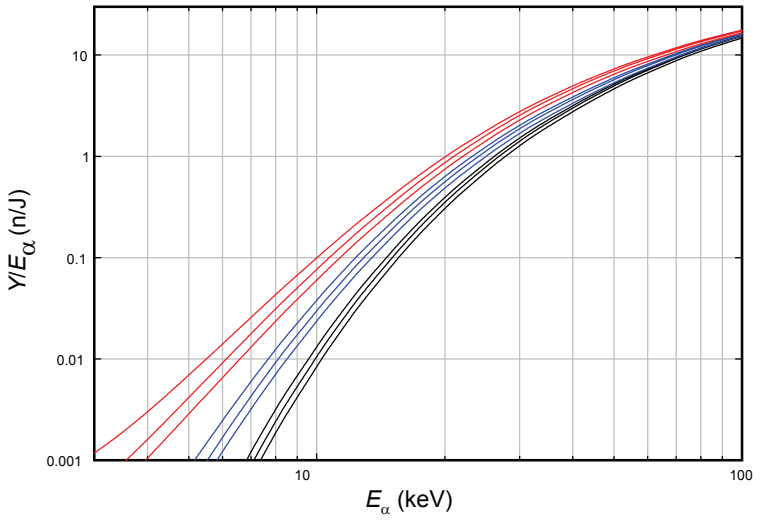

Figure 7. Secondary neutrons per alpha energy as a function of alpha energy. In the three top red curves, we have used $U_e(\mathrm{dd}) = 800$ eV; for the middle three blue curves, we have used $U_e(\mathrm{dd}) = 400$ eV; and for the bottom three black curves, we have used $U_e(\mathrm{dd}) = 0$ eV. In each case, we have run three cases with $U_e(\alpha\mathrm{d}) = 0, 800, 1600$ eV. The highest curve for each set of three corresponds to zero screening, and the lowest curve for each set corresponds to 1600 eV.

leads to about a factor of 2 difference in yield at 10 keV. The Rutherford scattering cross section is logarithmic in the alpha–deuteron screening distance, which accounts for weaker dependence on this screening parameter.

8. Discussion

As mentioned above, we were motivated to examine the secondary neutron yield due to energetic alpha particles due to the insistance of some of our colleagues, who are very good physicists, that energetic alpha particles can remain hidden in PdD. We can take advantage of the calculations presented above in order to estimate the upper limit on the alpha particle energy if it remains in PdD (or if it were to go into the D_2O electrolyte). From the experiments of Gozzi et al. [9], Takahashi et al. [10], and Scott et al. [11], we can extract upper limits on the number of neutrons per unit energy of excess heat produced to be 0.021, 0.01 and 0.008 n/J, respectively. The corresponding upper limit on the alpha particle energy is between 6200 and 7700 eV using a deuteron–deuteron screening energy of 800 eV. Assuming a deuteron–deuteron screening energy of 400 eV, the upper limit on the alpha energy is between 8200 and 9800 eV.

The experimental upper limits on the relative absence of neutrons, combined with the secondary neutron yields presented here, produces a very low upper limit on the alpha particle energy relative to the Q value from experiments (near 24 MeV). The simplistic proposals put forth by our physics colleagues are clearly inconsistent with experiment, since they would involve alpha particle energies well in excess of 1 MeV.

A preliminary version of these results and others appear in [12].

References

[1] A. Takahashi, T. Inokuchi, Y. Chimi, T. Ikegawa, N. Kaji, Y. Nitta, K. Kobayashi and M. Taniguchi, *Proc. ICCF5*, p. 69 (1995).
[2] P. L. Hagelstein, *J. Cond. Mat. Nucl. Phys.* **3** (2010) 35.
[3] T. Kambara, M. Takai, M. Nakamura and S. Kobayashi, *J. Phys. Soc. Japan* **44** (1978) 704.
[4] F. Raiola, L. Gang, C. Bonomo, G. Gyurky, M. Aliotta, H.W.Becker, R. Bonetti, C. Broggini, P. Corvisiero, A. D'Onofrio, Z. Fulop, G. Gervino, L. Gialanella, M. Junker, P. Prati, V. Roca, C. Rolfs, M. Romano, E. Somorjai, F. Streider, F. Terrasi, G. Fiorentini, K. Langanke and J. Winter, *Eur. Phys. J. A* **19** (2004) 283.
[5] F. C. Barker, *Nucl. Phys. A* **707** (2002) 277.
[6] M. La Cognata, A. Musumarra, C. Spitaleri, A. Tumino, C. Bonomo, S. Cherubini, P. Figuera, L. Lamia, M. G. Pellegriti, A. Rinolo, R. G. Pizzoni, C. Rolfs, S. Romano, D. Schürmann, F. Strieder, S. Tudisco and S. Typel, *Nucl. Phys. A* **758** (2005) 98c.
[7] K. Czerski, A. Huke, P. Heide and G. Ruprecht, *Eur. Phys. J. A* **27** (2006) 83.
[8] M. Griebel, S. Knapek and G. Zumbusch, *Numerical Simulation in Molecular Dynamics*, Springer, Berlin, 2000.
[9] D. Gozzi, R. Caputo, P. L. Cignini, M. Tomellini, G. Gigli, G. Balducci, E. Cisbani, S. Frullani, F. Garibaldi, M. Jodice and G. M. Urciuoli, *Proc. ICCF4*, Vol. 1, p. 2-1 (1994).
[10] A. Takahashi, A. Mega and T. Takeuchi, *Proc. ICCF3*, p.79 (1993).
[11] C. D. Scott, J. E. Mrochek, T. C. Scott, G. E. Michaels, E. Newman and M. Petek M, *Fusion Technol.* **18** (1990) 103.
[12] P. L. Hagelstein, *Naturwissenschaften* **97** (2010) 345.